Agronomy, Horticulture and Plant Science Faculty Publications

Department of Agronomy, Horticulture, and Plant Science

9-2013

Seed Burial Physical Environment Explains Departures from Regional Hydrothermal Model of Giant Ragweed (Ambrosia trifida) Seedling Emergence in U.S. Midwest

Adam S. Davis
USDA, Agricultural Research Service

Sharon Clay
South Dakota State University, sharon.clay@sdstate.edu

John Cardina
The Ohio State University

Frank Forcella
Kansas State University

John Lundquist
USDA, Agricultural Research Service

See next page for additional authors

Follow this and additional works at: https://openprairie.sdstate.edu/plant_faculty_pubs

Part of the Weed Science Commons

Recommended Citation

Authors

Adam S. Davis, Sharon Clay, John Cardina, Frank Forcella, John Lundquist, and Christy Sprague

Seed Burial Physical Environment Explains Departures from Regional Hydrothermal Model of Giant Ragweed (*Ambrosia trifida*) Seedling Emergence in U.S. Midwest

Adam S. Davis, Sharon Clay, John Cardina, Anita Dille, Frank Forcella, John Lindquist, and Christy Sprague*

Robust predictions of weed seedling emergence from the soil seedbank are needed to aid weed management. A common seed accession (Illinois) of giant ragweed was buried in replicate experimental gardens over 18 site years in Illinois, Michigan, Kansas, Nebraska, Ohio, and South Dakota to examine the importance of site and climate variability by year on seedling emergence. In a nonlinear mixed-effects modeling approach, we used a flexible sigmoidal function (Weibull) to model giant ragweed cumulative seedling emergence in relation to hydrothermal time accumulated in each site-year. An iterative search method across a range of base temperature (T_b) and base and ceiling soil matric potentials (ψ_b and ψ_c) for accumulation of hydrothermal time identified optima ($T_b = 4.4$ C, $\psi_b = -2,500$ kPa, $\psi_c = 0$ kPa) that resulted in a parsimonious regional model. Deviations between the fits for individual site-years and the fixed effects regional model were characterized by a negative relationship between random effects for the shape parameter *lrc* (natural log of the rate constant, indicating the speed at which emergence progressed) and thermal time (base 10 C) during the seed burial period October through March ($r = -0.51$, P = 0.03). One possible implication of this result is that cold winter temperatures are required to break dormancy in giant ragweed seeds. By taking advantage of advances in statistical computing approaches, development of robust regional models now is possible for explaining arable weed seedling emergence progress across wide regions.

Nomenclature: Giant ragweed, *Ambrosia trifida* L.

Key words: Abiotic influences on seed dormancy, hydrothermal time, nonlinear mixed effects models, regional environmental variation, seedling recruitment phenology.

Predicting weed emergence timing from the seedbank plays a critical role in scheduling early season POST weed management operations to achieve high efficacies by alerting farmers to upcoming phonological benchmarks for weed seedlings. For example, rotary hoeing is most effective when performed at the "white thread stage" of seedling development, after the weed seed germinates but before root establishment (Mt. Pleasant et al. 1994). The white thread stage is conceptualized easily for a single seedling, but this characterization is much more difficult for a population with variable phenology. Moreover, many POST herbicides have little soil activity and will not control weeds that have not yet emerged if applied too early. Conversely, if control techniques are applied too late, early emerging weeds may be too large for effective control (Carey and Kells 1995; Dalley et al. 2004). In addition, if weeds are controlled too late, crop yield potential already may have been reduced irreversibly even if the weeds are controlled (Clay et al. 2006; Moriles et al. 2012; Norsworthy and Oliveira 2004).

Models have been developed to predict temporal seedling emergence patterns for several weed species (Forcella 1998; Grundy and Mead 2000; Grundy et al. 2003; Hardegree and Winstral 2006; Oryokot et al. 1997a,b; Roman et al. 2000; Schutte et al. 2008). Seeds do not germinate if soil temperatures are too low and the first weed-emergence

prediction models developed used only air or soil temperature (thermal time). Thermal time in these studies was represented as growing degree days (GDD), such that

$$\text{GDD} = \sum \frac{T_{\min} + T_{\max}}{2} - T_b \qquad [1]$$

where $T_{\min}$ and $T_{\max}$ are daily minimum and maximum temperature, and T_b is a base temperature, below which thermal time units are not accumulated, optimized for the weed species of interest (Bewick et al. 1988). For example, WeedCast (Archer et al. 2006) uses a T_b of 4.4 C for summer annual weed species including common cocklebur (*Xanthium strumarium* L.), wild buckwheat (*Polygonum convolulus* L.), and giant ragweed, whereas the T_b reported for yellow foxtail [*Setaria pumila* (Poir.) Roemer & Schultes], barnyardgrass [*Echinochloa crus-galli* (L.) Beauv.], and common sunflower (*Helianthus annuus* L.) is 10 C. These data imply that giant ragweed and common cocklebur would emerge earlier in the growing season than common sunflower and barnyardgrass.

A more complex approach that often improves emergence predictions incorporates daily time-step models of soil water potential (ψ) along with soil temperature (Baskin and Baskin 1987; Gummerson 1986). Seeds cannot imbibe water from soils that are too dry and germination is delayed until enough water is present. The ψ can be measured directly using a psychrometer or other sensors. Environmental simulation models, such as the soil temperature and moisture model (STM^2) (Spokas and Forcella 2009), that calculate ψ from rainfall and inherent soil characteristics to adjust values based on infiltration estimates, clay, and organic matter content, have also been developed. In this second approach, the ψ data are then integrated with soil temperature into a single measurement designated as "hydrothermal time" (θ_{HT}) in which thermal time is only accumulated if soil matric potential is within a predetermined range. This method has been used successfully to model seedling emergence of many

* First author: Research Ecologist, U.S. Department of Agriculture–Agricultural Research Service (USDA-ARS) Global Change and Photosynthesis Research Unit, Urbana, IL 61801; second author: Professor, South Dakota State University, Brookings, SD, 57007; third author: Professor, Ohio Agricultural Research and Development Center, The Ohio State University, Wooster, OH, 44691; fourth author: Associate Professor, Kansas State University, Manhattan, KS, 66506; fifth author: Research Agronomist, USDA-ARS North Central Soil Conservation Research Laboratory, Morris, MN, 56267; sixth author: Professor, University of Nebraska, Lincoln, NE, 68583; seventh author: Associate Professor, Michigan State University, East Lansing, MI, 48824. Corresponding author's E-mail: adam.davis@ars.usda.gov

broadleaf and grass species at various locations worldwide (Forcella 1998; Forcella et al. 2000; Gardarin et al. 2010; Grundy 2003; Grundy et al. 2003; Gummerson 1986; Masin et al. 2010; Oryokot et al. 1997a; Roman et al. 2000; Spokas and Forcella 2009).

Weed seedling emergence models have often been challenged by spatiotemporal variability. For example, Grundy et al. (2003) reported that a single generic model could not predict emergence of common chickweed [*Stellaria media* (L.) Vill.] from different origins under different climatic conditions even though the seeds were planted in a common substrate. Giant ragweed seeds from Illinois, Iowa, and Michigan that were sown in a common garden gave rise to seedlings that differed in their patterns of emergence (Johnson et al. 2007), likely because of preexisting and differential dormancy states of the harvested seeds. Populations of giant ragweed from Ohio (eastern U.S. Corn Belt) appear to have adapted to glyphosate-based management systems in corn and soybean by delayed emergence. Early- and late-emerging biotypes had emergence lag periods of 60 and 600 degree days, respectively (Schutte et al. 2008). Differing degrees of seed dormancy among biotypes has been proposed as one possible explanation for differential emergence timing among these populations (Schutte et al. 2012). However, the models developed by Schutte et al. (2008) for seedling responses to soil θ_{HT} of each biotype did not encompass possible effects of soil θ_{HT} on seed dormancy.

We propose that two impediments to the development of unified models of spatiotemporally diverse seedling emergence data have been (1) the lack of appropriate statistical methods and (2) inattention to differential abiotic influences on seed dormancy. Previous modeling attempts have relied on least squares nonlinear regression modeling techniques in which all model parameters were treated as fixed effects (Grundy et al. 2003; Ratkowski 1983). The recent development of nonlinear mixed effects modeling approaches (Pinheiro and Bates 2004) offers unprecedented flexibility in describing the nonlinear behavior of large groups of related, but variable, sets of observations. In this approach, a single biological process model (e.g., sigmoidal emergence response function based on accumulation of soil hydrothermal time) is fit to all site-years, estimating both fixed effects (across site-years) and random effects (within site-years) for model parameters. Benefits of such an approach include the following: 1) linking all observations to a common model, with a single prior distribution for the fitted model that permits linked inferences to be made; 2) improved inference space, since random effects in the model are treated as draws from a larger, unobserved, pool of phenomena; and 3) potential for iterative improvement of the basic process model, as unexplained environmental variation discovered in the random effects may guide further model refinement (Luschei and Jackson 2005).

Although seed dormancy is a well-known influence on the timing and extent of seedling emergence (Benech-Arnold et al. 2000), most models for summer annual weeds implicitly assume that overwintering relieves all traces of dormancy possessed by seeds in the soil. This assumption likely is true in many situations, but may be inaccurate in others. For instance, models for seedling emergence of large crabgrass [*Digitaria sanguinalis* (L.) Scop.] were improved when hypothetical seed dormancy was broken by altering the models to include several cycles of diurnal soil temperature fluctuations > 6 C prior to the start of seed germination

(Forcella et al. 2000). Inclusion of dormancy relief functions in emergence models of summer annual weeds is expected to be especially useful when comparing field-based data over wide geographic areas that probably experienced highly variable overwinter soil microclimates.

Here we report the results of a field study of giant ragweed seedling emergence over 18 site-years in eight locations in the north central region of the United States. Our objective was to quantify the seedling emergence dynamics over a wide enough range of environmental conditions to develop a robust statistical model identifying critical abiotic drivers explaining variation in this process at a regional scale.

Materials and Methods

Seed Accessions and Site Information. Giant ragweed seeds were collected from Urbana, IL, in autumn just after seed maturity. In 2005, seeds were collected from a riparian population situated in a riverbank field margin (''riparian'' accession), whereas in 2006 and 2007, seeds were collected from giant ragweed populations occurring within a maize field located at the University of Illinois Crop Sciences Research and Education Center (''arable'' accession). Mature plants were air-dried in a sheltered area for 2 wk, after which any dehisced seeds were collected and cleaned to remove chaff and light seed. Seed lots were assessed for initial viability using tetrazolium staining methods (AOSA 2000). Clean seed was distributed to participants and planted at field locations at Savoy, IL (40.05°N; 88.24°W); East Lansing (42.71°N; 84.47°W) and St. Charles (43.31°N; 84.13°W), MI; Manhattan, KS (39.19°N; 96.6°W); Ithaca, NE (41.17°N, 96.41°W); Wooster, OH (40.78°N, 81.92°W); and Aurora, SD (44.29°N; 96.65°W).

Specific experimental design and other site information are presented in Wortman et al. (2012). Briefly, at each location, in four replicate plots, 100 seeds were placed into 12 by 12–cm wire mesh baskets filled with 2 cm of topsoil from the plot area and buried so that the soil surface in the baskets was flush with the surrounding soil surface. Seeds were sown in mid-October of the year of collection to allow for natural overwinter cold treatment. Eighteen site-years of data were obtained for giant ragweed emergence (3 yr from IL, MI (two locations), and KS [2006 to 2008] and 2 yr from NE, OH, and SD [2007, 2008]). Weekly destructive seedling emergence counts were performed. Monitoring began in late February, before emergence occurred at any location, and continued through late August, well after emergence had ended (Figure 1).

Soil Microclimate Conditions. Hourly air temperatures and rainfall, along with other meteorological data, were collected at weather stations within 10 km of each study site. STM[2] (Spokas and Forcella 2009) was then used to model soil T and ψ at 2 cm based on solar radiation, soil properties (sand, silt, clay, organic matter contents), latitude, longitude, and elevation of the field site, along with daily minimum and maximum air temperatures and daily precipitation to simulate microclimate conditions.

Calculating θ_{HT}. We modeled various time series of daily accumulation of θ_{HT} corresponding to selected combinations of T_b, ψ_b (below which soil was considered too dry to
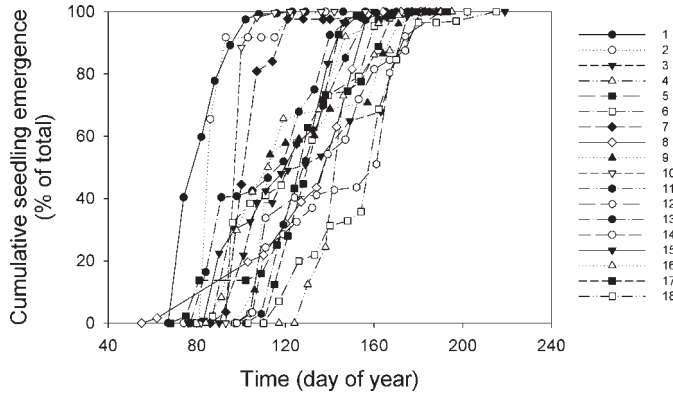
Figure 1. Cumulative giant ragweed seedling emergence, by day of year, for 18 site-years across the north central Corn Belt of the United States. Site-year codes are as follows: 1 to 3 = Savoy, IL, 2006 to 2008; 4 to 6 = Manhattan, KS, 2006 to 2008; 7 to 9 = East Lansing, MI, 2006 to 2008; 10 to 12 = St. Charles, MI, 2006 to 2008; 13 and 14 = Mead, NE, 2007 to 2008; 15 and 16 = Wooster, OH, 2007 to 2008; 17 and 18 = Aurora, SD, 2007 to 2008.

Figure 2. Goodness of fit of saturated seedling emergence model to variation in base temperature (T_b: 1, 2, 4.4, and 5 C) and soil matric potential (ψ) threshold values for a) hydrothermal time (threshold value of ψ_b) and b) modified hydrothermal time (threshold value of ψ_c) models. Modified hydrothermal time models (those including both a base and ceiling soil matric potential threshold) all used a ψ_b of −2,500 kPa. AIC = Akaike's information criterion.

accumulate thermal time), and ψ_c (above which soil was considered too wet to accumulate thermal time) chosen to bracket the range of those found in the literature on giant ragweed seedling emergence (Archer et al. 2006; Schutte et al. 2008). Values of T_b included 1, 2, 4.4, and 5 C, values of ψ_b included −20,000, −10,000, −5,000, −2,500, −1,000, −100, and −33 kPa, and values of ψ_c included −40, −33, −10, −1, and 0 kPa. Note that θ_{HT} calculated with $\psi_b =$ −20,000 kPa and $\psi_c = 0$ was equivalent to thermal time (unmodified by soil moisture constraints), since soil ψ did not drop below this value for any of the modeled site-years. Although not previously used in θ_{HT} calculations associated with seedling emergence, ψ_c was included in this study to determine whether soil conditions could be too wet (i.e., anoxic) to permit giant ragweed seedling emergence. For each site-year, January 1 was treated as $\theta_{HT} = 0$ (with the exception of KS-2006, when giant ragweed seeds were buried in the soil on March 1, and treated as $\theta_{HT} = 0$ for this site-year). We accumulated θ_{HT} as

$$\theta_{HT} = \sum_{i=1}^{n} \theta_{H_i} \theta_{T_i} \qquad [2]$$

where i = day of year at a particular location, n = final observation day of year at a particular location, θ_H = soil matric potential in relation to ψ_b, and θ_T = soil temperature. When $\psi_c > \psi > \psi_b$, $\theta_H = 1$, or else $\theta_H = 0$ when $\psi < \psi_b$ or $\psi > \psi_c$; θ_T is calculated according to equation 1.

Statistical Modeling. Our approach to modeling the seedling germination dynamics of giant ragweed in response to θ_{HT} was accomplished in several steps: 1) finding optimal base values for incrementing θ_{HT} with respect to a saturated statistical model, 2) performing model simplification at the optimal base values for θ_{HT}, and 3) analyzing associations among random effects for the most parsimonious θ_{HT} model and environmental variation across site-years.

At the core of our statistical modeling approach to quantifying regional seedling germination dynamics of giant ragweed was a nonlinear mixed effects modeling framework, fit by maximum likelihood methods (Pinheiro and Bates 2004). The saturated model containing fixed and random effects for all parameters of the Weibull equation (Ratkowski
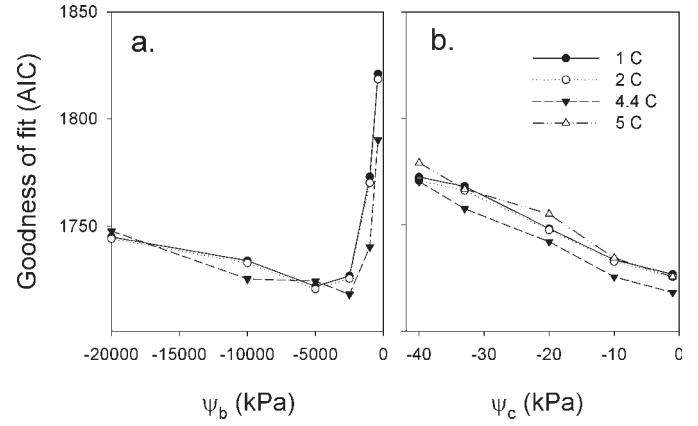
1983), a flexible mathematical function used to describe cumulative data series, was formulated such that

$$y_i \sim (\beta_{1i} + b_{1i}) - (\beta_{2i} + b_{2i}) * e^{\left[\left(-e^{(\beta_{3i} + b_{3i})}\right)\left(\theta_{HT_i}{}^{(\beta_{4i} + b_{4i})}\right)\right]} + \varepsilon_i$$

$$b_1 \sim N(0, \psi), \quad \varepsilon_i \sim N(0, \sigma^2)$$

$$\psi = \begin{bmatrix} \sigma_{11} & 0 & 0 & 0 \\ 0 & \sigma_{22} & 0 & 0 \\ 0 & 0 & \sigma_{33} & 0 \\ 0 & 0 & 0 & \sigma_{44} \end{bmatrix} \qquad [3]$$

where i = experimental unit; y = cumulative percent emergence at a cumulative θ_{HT} value; β_1 and b_1 represent the fixed and random effects, respectively, for *Asym*, the upper horizontal asymptote (theoretical maximum for Y normalized to 100%); β_2 and b_2 represent the fixed and random effects, respectively, for *Drop*, the vertical distance between the upper and lower horizontal asymptotes; β_3 and b_3 represent the fixed and random effects, respectively, for *lrc*, the natural log of the rate of increase; β_4 and b_4 represent the fixed and random effects, respectively, for *pwr*, a curve shape parameter; and ε_i represents the error term (Ratkowski 1983). This mixed effects model contains eight parameters to be estimated; in comparison, a fixed-effects-only approach in which individual models were fit to each site-year of data would result in an overparameterized model, with $4 \times 18 = 72$ parameters to be estimated. We chose a diagonal covariance structure for the random error terms because a general positive-definite Log-Cholesky covariance structure (including all factorial combinations of random effects associations) did not converge for these data (Pinheiro and Bates 2004).

The search for optimal base values for the saturated θ_{HT} model and subsequent model simplification were implemented using a maximum likelihood model selection approach in the *nlme* package of R version 12.13.0 (R Development Core Team, Vienna, Austria. Support from the data for competing models was evaluated on the minimization of maximum likelihood criteria including Akaike information criterion (AIC) and Bayesian information criterion (BIC), and through

Table 1. Maximum likelihood selection among best nonlinear mixed effects models of giant ragweed cumulative seedling emergence following a Weibull response function to hydrothermal time (base temperature = 4.4 C, base soil water potential = −2,500 kPa).

Model	Fixed effects[a]	Random effects	df[b]	AIC	BIC	LL	w_i
1	$Asym + Drop + lrc + pwr \sim 1$	$Asym + Drop + lrc + pw \, r\sim 1$	9	1,718	1,749	−851	2.8×10^{-5}
2	$Asym + Drop + lrc + pwr \sim 1$	$lrc \sim 1$	6	1,750	1,771	−869	3.2×10^{-12}
3	$Asym + Drop + lrc + pwr \sim 1$	$Drop + lrc \sim 1$	8	1,717	1,744	−850	4.6×10^{-5}
4	$Asym \sim 1, Drop + lrc + pwr \sim$ accession	$Drop + lrc \sim 1$	11	1,699	1,736	−839	0.38
5	$\mathbf{Asym + Drop \sim 1, lrc + pwr \sim accession}$	$\mathbf{Drop + lrc \sim 1}$	**10**	**1,698**	**1,732**	**−838**	**0.62**
6	$Asym + Drop + pwr \sim 1, lrc \sim$ accession	$Drop + lrc \sim 1$	9	1,716	1,747	−849	7.7×10^{-5}
7	$Asym + Drop \sim 1, lrc + pwr \sim$ accession	$lrc \sim 1$	8	1,721	1,749	−853	6.3×10^{-6}

[a] Weibull function parameters treated as fixed effects: *Asym*, upper horizontal asymptote; *Drop*, vertical difference between upper and lower horizontal asymptotes; *lrc*, ln(rate constant); *pwr*, shape parameter. The symbol ~ 1 indicates that fixed effects refer to model intercepts only, whereas the symbol ~ accession indicates that a fixed effect quantifies differences between factor levels.

[b] Model selection criteria abbreviations: df, degrees of freedom; AIC, Akaike's information criterion; BIC, Bayesian information criterion; LL, log likelihood; w_i, Akaike weights. For AIC and BIC, smaller values indicate more parsimonious models, whereas for LL, larger values indicate more parsimonious models. Akaike weights range from 0 to 1, sum to 1 for a group of candidate models, and indicate the probability that a given model represents the most parsimonious model (shown in bold) within the group.

Akaike weights (the probability that a given model was the best among the pool of candidate models) (Burnham and Anderson 2002). Simple and partial correlations between fitted random effects for parameters of the most parsimonious θ_{HT} seedling emergence model and environmental variables (soil T, soil GDD$_{10}$, soil ψ and rainfall) during overwinter seed burial (October through March) and during seedling emergence (period from first recorded seedling emergence to cessation of emergence) were implemented in the *corpcor* package of R version 12.13.0.

Results and Discussion

Base Values for θ_{HT} Model. The search for optimal base values for the θ_{HT} model of giant ragweed seedling emergence values identified clear optima for each soil property threshold. In approaching these optima, variation in ψ appeared to have more influence than variation in T_b (Figure 2). Based on minimization of AIC, the best fit of the saturated model to the data occurred when θ_{HT} was accumulated with $T_b = 4.4$ C and $\psi_b = -2,500$ kPa (Figure 2a). Placing a restriction on ψ_c did not improve model performance (Figure 2b). The special condition of overly wet soils inhibiting giant ragweed seedling emergence was therefore removed from further consideration during model selection.

Our optimal T_b value of 4.4 C corresponds to the empirical optimum found by Archer et al. (2006). This was considerably warmer than the T_b value of 2 C used by Schutte et al. (2008), which was extrapolated from the literature. The issue of optimal T_b will be discussed further in "Environmental Variation Unexplained by θ_{HT}."

Lack of effect of saturated soils (with high ψ values) on giant ragweed seedling emergence may not be surprising given that

it is a riparian-adapted species. More interesting is the very low optimum ψ_b at which θ_{HT} for giant ragweed seedling emergence continued to accumulate. This was well below the soil matric potential representing the permanent wilting point for plants, $\psi = -1,500$ kPa. Giant ragweed seeds are apparently able to imbibe and retain sufficient water over the pregermination burial period, even under very dry conditions, to drive the seedling emergence process. Since our emergence counting process was destructive, we did not follow the impact of dry soil on seedling survival to reproductive maturity.

Model Selection. Although seedling emergence progress varied widely among site-years when viewed by day of year (Figure 1), we were able to construct a unifying θ_{HT} model to describe giant ragweed seedling emergence using a nonlinear mixed effects modeling approach. Maximum-likelihood selection among seven nested candidate models, derived from the saturated model, indicated strong support for model 5 (Table 1). Akaike weights for model 5 indicated a 62% probability that this was the most parsimonious model among the pool of candidate models. The fixed-effects structure of this model consisted of fixed intercepts for β_1 (*Asym*) and β_2 (*Drop*) and categorical fixed effects of *accession* for β_3 (*lrc*) and β_4 (*pwr*) (Table 2). The random effects structure of this model contained terms only for b_2 (*Drop*) and b_3 (*lrc*). Parameter estimates for model 5 are given in Table 2. Given that this model is able to make predictions for all site-years of data, while lowering prediction error in comparison to other θ_{HT} models considered or the day-of-year emergence model, we consider model 5 to represent a robust model for predicting giant ragweed seedling emergence for the north central Corn Belt.

Table 2. Summary of random and fixed effects for the most parsimonious nonlinear mixed effects model of giant ragweed cumulative seedling emergence following a Weibull response function to hydrothermal time (base temperature: 4.4 C, base soil water potential = −2,500 kPa).

Fixed effects[a]	Coefficient	SE	df	*t*-value	P-value	Random effects	SD
Asym	99.8	1.0	206	96.1	0.0001	*Drop*	11.4
Drop	105.7	3.8	206	28.1	0.0001	*lrc*	1.2
lrc (arable)	−12.7	0.8	206	−16.3	0.0001	residual	7.3
lrc (riparian)	−6.2	1.9	206	−3.2	0.0016		
pwr (arable)	2.0	0.11	206	18.0	0.0001		
pwr (riparian)	1.38	0.36	206	3.9	0.0001		

[a] Explanation of fixed effects parameters: *Asym*, upper horizontal asymptote; *Drop*, vertical difference between upper and lower horizontal asymptotes; *lrc*, ln(rate constant); *pwr*, shape parameter. The parameters *Asym* and *Drop* are modeled only as intercepts, whereas the parameters *lrc* and *pwr* are modeled with respect to the factor "accession" (with the arable accession of giant ragweed represented by the intercept, and the riparian accession of giant ragweed represented as a shift to the intercept).
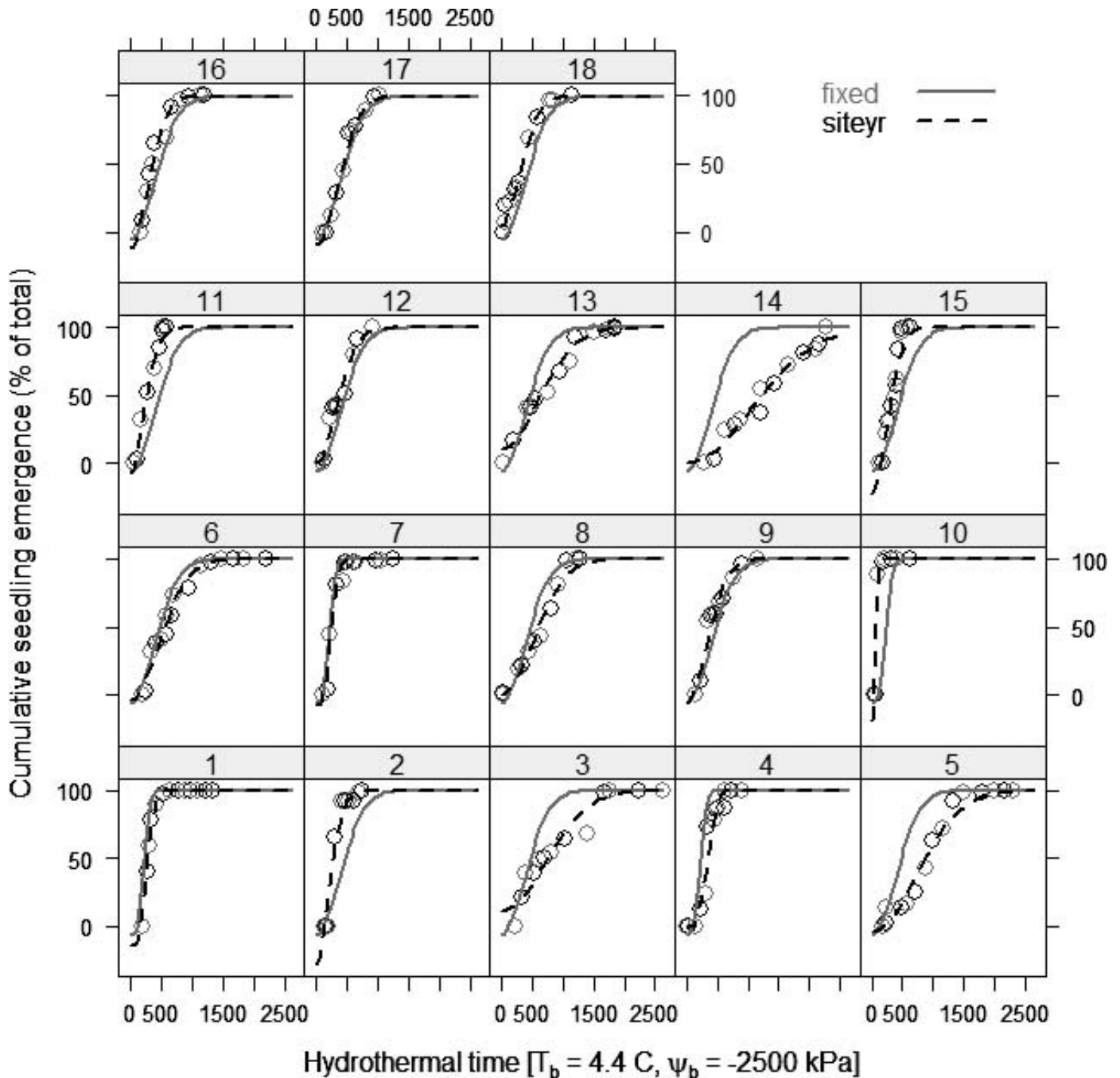
Figure 3.   Fixed (solid grey lines) and random (site-year; dashed black lines and empty circles) effects for nonlinear mixed effects Weibull model of giant ragweed seedling emergence for 18 site-years across the north central Corn Belt of the United States. Site-year codes are as follows: 1 to 3 = Savoy, IL, 2006 to 2008; 4 to 6 = Manhattan, KS, 2006 to 2008; 7 to 9 = East Lansing, MI, 2006 to 2008; 10 to 12 = St. Charles, MI, 2006 to 2008; 13 and 14 = Mead, NE, 2007 tpk 2008; 15 and 16 = Wooster, OH, 2007 to 2008; 17 and 18 = Aurora, SD, 2007 to 2008. The riparian accession of giant ragweed was used in site-years 1,4, 7, and 10; all other site years used the arable accession. Base values for accumulating hydrothermal time were base temperature = 4.4 C and base soil water potential = −2,500 kPa.

Giant ragweed seed accession had a significant effect on both *lrc* and *pwr* (Table 2). Effects of *accession* on *pwr*, a shape parameter, indicate that the seedling emergence curves had a different shape for the riparian and arable seed accessions. In contrast, *accession* effects on *lrc* (natural log of the rate constant) have a more precise biological meaning, since the rate constant (*c*) describes the speed at which the emergence process is unfolding (larger values of *c* corresponding to a faster process). Back-transforming from the parameter estimates, $c_{riparian} = 2.0 \times 10^{-3}$ and $c_{arable} = 3.1 \times 10^{-6}$. The rate constant is larger for the riparian accession,

indicating that the seedling emergence process proceeds more rapidly for this accession.

Visual inspection of the fitted *nlme* model (Figure 3) shows that the germination dynamics are consistent with the quantitative inference that seedling emergence proceeds more swiftly in the riparian accession (site-years 1, 4, 7, 10) than in the arable accession (site-years 2, 3, 5, 6, 8, 9, 11 to 18). This corroborates other reports that giant ragweed seedling emergence phenology varies with provenance (Johnson et al. 2007), with naturally occurring successional populations in riparian areas emerging in an earlier, narrower germination
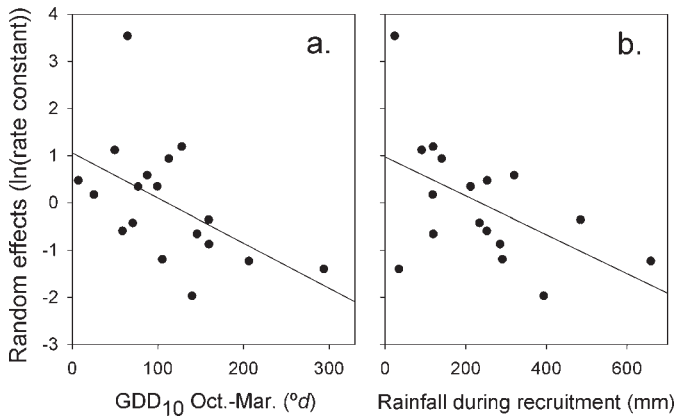
Figure 4. Association between estimated random effects for the parameter *lrc* (ln[rate constant]) and a) thermal time (GDD_{10}) accumulated during the overwinter seed burial period from October through March, and b) rainfall during seedling recruitment.

window, and populations from upland disturbed areas emerging over an extended time period (Schutte et al. 2012). The extended germination biotype of giant ragweed occurring in arable fields presumably was selected by agricultural soil disturbance and weed management operations, resulting in a bet-hedging seedling emergence strategy to avoid local extinction due to early-season agricultural management. We did not observe biphasic seedling emergence from any of the three giant ragweed populations in our study, in contrast to the observations of Schutte et al. (2012), who documented this emergence behavior in several seed accessions among 14 different successional and arable populations in Ohio.

Environmental Variation Unexplained by θ_{HT}. We examined the relationship between fitted random effects for model parameters and environmental variables (air temperature, GDD_1, GDD_2, $GDD_{4.4}$, GDD_{10}, and rainfall) during seed burial and during seedling emergence. Random departures from the fixed model for *lrc* were most strongly associated with GDD_{10} during overwinter seed burial ($GDD_{10\_Oct–Mar}$) and rainfall during the seedling emergence period (g_{ppt}). There were negative correlations between random effects for *lrc* and both $GDD_{10\_Oct–Mar}$ ($r = -0.51$, $P = 0.03$), and g_{ppt} ($r = -0.52$, $P = 0.03$) (Figure 4). Although these quantitative associations were similar, partial correlation analysis indicated that they were not an artifact of any correlation between $GDD_{10\_Oct–Mar}$ and g_{ppt} [pcorr$_{lrc*GDD10\_Oct–Mar}$ (g_{ppt}) $= -0.48$, $P = 0.04$; pcorr$_{lrc*g_{ppt}(GDD10\_Oct–Mar)}$ $= -0.48$, $P = 0.04$]. Significant associations did not exist between random effects for *lrc* and thermal time accumulated with lower base temperatures ($T_b = 1$, 2, or 4.4 C).

Based on the negative relationship between random effects for *lrc* and g_{ppt}, we can surmise that either we did not fully capture the effects of soil moisture variation during seedling emergence with the θ_{HT} model, or that precipitation during the seedling emergence period may have influenced emergence phenology in other ways. For example, more rainy days during the seedling emergence period may have resulted in greater cloud cover and less incident solar radiation at the soil surface to stimulate seedling emergence.

The negative relationship between random effects for *lrc* and $GDD_{10\_Oct–Mar}$ has implications for both giant ragweed

seed biology and future seedling emergence modeling efforts. First, it indicates that warm soils during the overwinter seed burial period had a cumulative effect on giant ragweed germination status, slowing the seedling emergence process, which supports the conclusions of Schutte et al (2012) that giant ragweed seed dormancy loss occurs in response to cold, moist conditions overwinter. More specifically, Ballard et al. (1996) observed in laboratory settings that seed dormancy of giant ragweed was not lost when stratified at 8 C but was within 60 d at 4 C. These observations find additional support from controlled environment studies showing that seed incubation environment temperature in certain species is linked to the kinetics of dormancy loss and base temperature of subsequent seedling emergence (Steadman and Pritchard 2004). That this finding is echoed in our observational field study indicates that future models of giant ragweed (and perhaps other species as well) seedling emergence should incorporate a process model for the pregermination soil burial period. To build such a model will require controlled environment studies, resembling those of Steadman and Pritchard (2004), to develop dose-response curves linking cumulative thermal time in the seed burial environment and T_b for seedling emergence.

Literature Cited

[AOSA] Association of Official Seed Analysts. 2000. Tetrazolium testing handbook. Contribution No. 29 to the Handbook on Seed Testing. 302 p.

Archer, D. W., F. Forcella, A. Korth, A. Kuhn, J. Eklund, and K. Spokas. 2006. WeedCast. http://www.ars.usda.gov/services/software/download.htm?softwareid =112. Accessed June 20, 2012.

Ballard, T. O., M. E. Foley, and T. T. Bauman. 1996. Germination, viability, and protein changes during cold stratification of giant ragweed (*Ambrosia trifida* L.) seed. J. Plant Physiol. 149:229–232.

Baskin, J. M. and C. C. Baskin. 1987. Environmentally induced changes in the dormancy states of buried weed seeds. Pages 695–706 in Proceedings of British Crop Protection Conference: Weeds. Brighton, UK: British Crop Protection Council.

Benech-Arnold, R. L., R. A. Sanchez, F. Forcella, B. C. Kruck, and C. M. Ghersa. 2000. Environmental control of dormancy in weed seed banks in soil. Field Crops Res. 67:105–122.

Bewick, T. A., L. K. Binning, and B. Yandell. 1988. A degree day model for predicting the emergence of swamp dodder in cranberry. J. Am. Soc. Hortic. Sci. 113:839–841.

Burnham, K. P. and D. R. Anderson. 2002. Model Selection and Inference: A Practical Information-Theoretic Approach. 2nd ed. New York: Springer Verlag. Pp. 32–74.

Carey, J. B. and J. J. Kells. 1995. Timing of total postemergence herbicide applications to maximize weed control and corn yield. Weed Technol. 9:356–361.

Clay, S. A., K. R. Banken, F. Forcella, M. M. Ellsbury, D. E. Clay, and A. E. Olness. 2006. Influence of yellow foxtail on corn growth and yield. Commun. Soil Sci. Plant Anal. 37:1421–1435.

Dalley, C. D., J. J. Kells, and K. A. Renner. 2004. Effect of glyphosate application timing and row spacing on corn (*Zea mays*) and soybean (*Glycine max*) yields. Weed Technol. 18:165–176.

Forcella, F. 1998. Real-time assessment of seed dormancy and seedling growth for weed management. Seed Sci. Res. 8:201–209.

Forcella, F., R. L. Benech-Arnold, R. Sanchez, and C. M. Ghersa. 2000. Modeling seedling emergence. Field Crops Res. 67:123–139.

Gardarin, A., J. P. Guillemin, N. M. Munier-Jolain, and N. Colbach. 2010. Estimation of key parameters for weed population dynamics models: base temperature and base water potential for germination. Eur. J. Agron. 32:162–168.

Grundy, A. C. 2003. Predicting weed emergence: a review of approaches and future challenges. Weed Res. 43:1–11.

Grundy, A. C. and A. Mead. 2000. Modeling weed emergence as a function of meteorological records. Weed Sci. 48:594–603.

Grundy, A. C., N.C.B. Peters, I. A. Rasmussen, K. M. Hartmann, M. Sattin, L. Andersson, A. Mead, A. J. Murdoch, and F. Forcella. 2003. Emergence of *Chenopodium album* and *Stellaria media* of different origins under different climatic conditions. Weed Res. 43:163–176.

Gummerson, R. J. 1986. The effect of constant temperature and osmotic potentials on the germination of sugar beet. J. Exp. Bot. 37:729–741.

Hardegree, S. P. and A. H. Winstral. 2006. Predicting germination response to temperature. II. Three-dimensional regression, statistical gridding and iterative-probit optimization using measured and interpolated-subpopulation data. Ann. Bot. 98:403–410.

Johnson, B., M. Loux, D. Nordby, C. Sprague, G. Nice, A. Westhoven, and J. Stachler. 2007. Biology and Management of Giant Ragweed. GWC-12. Purdue University Extension. 16 p www.ces.purdue.edu/new. Accessed June 20, 2012.

Luschei, E. C. and R. D. Jackson. 2005. Research methodologies and statistical approaches for multitactic systems. Weed Sci. 53:393–403.

Masin, R., D. Loddo, S. Benvenuti, M. C. Zuin, M. Macchia, and G. Zanin. 2010. Temperature and water potential as parameters for modeling weed emergence in central-northern Italy. Weed Sci. 58:216–222.

Moriles, J., S. Hansen, D. P. Horvath, G. Reicks, D. E. Clay, and S. A. Clay. 2012. Microarray and growth analyses identify differences and similarities of early corn response to weeds, shade, and nitrogen stress. Weed Sci. 158–166.

Mt. Pleasant, J., R. F. Burt, and J. C. Frisch. 1994. Integrating mechanical and chemical weed management in corn (*Zea mays*). Weed Technol. 8:217–223.

Norsworthy, J. K. and M. J. Oliveira. 2004. Comparison of the critical period for weed control in wide- and narrow-row corn. Weed Sci. 52:802–807.

Oryokot, J.O.E., L. A. Hunt, S. D. Murphy, and C. J. Swanton. 1997a. Simulation of pigweed (*Amaranthus* spp.) seedling emergence in different tillage systems. Weed Sci. 45:684–690.

Oryokot, J.O.E., S. D. Murphy, and C. J. Swanton. 1997b. Effect of tillage and corn on pigweed (*Amaranthus* spp.) seedling emergence and density. Weed Sci. 45:120–126.

Pinheiro, J. C. and D. M. Bates. 2004. Mixed-Effects Models in S and S-PLUS. New York: Springer. 528 p.

Ratkowsky, D. A. 1983. Nonlinear Regression Modeling: A Unified Practical Approach. New York: Marcel Dekker. Pp. 135–153.

Roman, E. S., S. D. Murphy, and C. J. Swanton. 2000. Simulation of *Chenopodium album* seedling emergence. Weed Sci. 48:217–224.

Schutte, B. J., E. E. Regnier, and S. K. Harrison. 2012. Seed dormancy and adaptive seedling emergence timing in giant ragweed (*Ambrosia trifida*). Weed Sci. 60:19–26.

Schutte, B. J., E. E. Regnier, S. K. Harrison, J. T. Schmoll, K. Spokas, and F. Forcella. 2008. A hydrothermal seedling emergence model for giant ragweed (*Ambrosia trifida*). Weed Sci. 56:555–560.

Spokas, K. and F. Forcella. 2009. Software tools for weed seed germination modeling. Weed Sci. 57:216–227.

Steadman, K. J. and H. W. Pritchard. 2004. Germination of *Aesculus hippocastanum* seeds following cold-induced dormancy loss can be described in relation to a temperature-dependent reduction in base temperature (Tb) and thermal time. New Phytol. 161:415–425.

Wortman, S. E., A. S. Davis, B. J. Schutte, J. L. Lindquist, J. Cardina, J. Felix, C. L. Sprague, J. A. Dille, A.H.M. Ramirez, G. Reicks, and S. A. Clay. 2012. Local conditions, not spatial gradients, drive demographic variation of *Ambrosia trifida* and *Helianthus annuus* across northern U.S. maize belt. Weed Sci. 60:440–450.